IAA-AAS-DyCoSS2-05-08

STABILITY OF ORBITS NEAR LARGE MASS RATIO BINARY SYSTEMS

Natasha Bosanac,[*] Kathleen C. Howell[†] and Ephraim Fischbach[‡]

With recent scientific interest into the composition, origin and dynamical environment of small bodies in the solar system, binary asteroids present a potential target for manned and robotic missions. In this investigation, periodic motions near a large mass ratio binary are explored within the context of the circular restricted three-body problem. Specifically, stability analysis is used to evaluate the effect of the mass ratio on the structure of families of periodic orbits. Such analysis is useful in a variety of applications, including trajectory design in a binary asteroid system or determining possible motions for exoplanets in the vicinity of binary star systems.

INTRODUCTION

With recent scientific interest into the composition, origin and dynamical environment of small bodies in the solar system, asteroids have become the target of an increasing number of manned and robotic mission concepts. Among the expansive array of asteroids that have been observed and catalogued, approximately 16% are members of binary or triple systems, none of which have yet been visited by a spacecraft.[1] Many of these observed binaries possess significantly larger mass ratios than pairs in the Sun-planet and planet-moon systems commonly examined within the solar system. In addition, the absolute mass of each companion may not be accurately inferred from orbit observations without further information about the composition of the asteroid. Similar uncertainties also occur in mass estimates for bodies that exist beyond the solar system, including binary star systems with large mass ratios. Since the dynamical environment in the vicinity of a binary is inherently chaotic, uncertainties in the relative mass of each body may significantly affect the trajectory followed by a small object.

In this investigation, periodic motions of a spacecraft in the vicinity of a large mass ratio binary system are explored within the context of the circular restricted three-body problem. Although asteroids possess irregular shapes, the restricted problem offers a reasonable approximation to higher-order gravitational models. In other studies, this simplified model has proven invaluable in a preliminary exploration of the infinite variety of behaviors that a spacecraft can exhibit within a binary system.[2] Of particular interest are periodic orbits, which contribute to an underlying structure including the potential for attracting or repelling trajectories in their vicinity. Accordingly, an analysis of the stability of families of orbits in the restricted problem can be employed to guide trajectory design. For instance, stable orbits might be preferred for long scientific observation of a binary asteroid. If there are significant uncertainties in the companion masses and the orbital stability is not observed to be sensitive to the mass ratio, the corresponding orbit may be a good candidate for further analysis in higher-fidelity models. Similar analysis could also be insightful to identify possible pathways for capture of an exoplanet around a binary star. In such extrasolar systems, the masses of the

[*]Ph.D. Student, School of Aeronautics and Astronautics, Purdue University, 701 W. Stadium Ave., West Lafayette, IN, 47906, USA.
[†]Hsu Lo Distinguished Professor of Aeronautics and Astronautics, School of Aeronautics and Astronautics, Purdue University, 701 W. Stadium Ave., West Lafayette, IN, 47906, USA.
[‡]Professor of Physics, Department of Physics and Astronomy, Purdue University, 525 Northwestern Ave., West Lafayette, IN, 47906, USA.

two stars are often approximated from observational data, and may vary over time due to mass exchange, producing an uncertainty in the mass ratio. Additionally, stability analysis is also used to locate a bifurcation along a family of orbits, which can indicate either a structural change or the formation of a new family. If a well-known family of orbits disappears at a nearby mass ratio, it might not exist for the true masses in the target binary system. The detection of a new family of orbits may offer alternative options for examination that are both insensitive to changes in the mass ratio and satisfy a given set of requirements.

To visualize the stability across a given family of orbits at various mass ratios, a two-dimensional representation, similar to an exclusion plot, is employed. Exclusion plots are often used in physics to depict constraints on combinations of parameters.[3] This concept is extended to represent the stability of periodic orbits in the vicinity of binary systems, with each orbit characterized by two parameters: the orbital period and the mass ratio. From Floquet's theorem, reciprocal pairs of eigenvalues are frequently employed to qualitatively classify the stability of a periodic orbit. Through analysis of the stability index, i.e., the sum of each pair of eigenvalues, three cases emerge: stability, positive instability and negative instability.[4] Each periodic orbit can, therefore, be represented on an exclusion plot as a point colored by the type of linear stability it exhibits. The resulting composite stability representation corresponding to a specified family, over a range of mass ratios, offers a simple visualization of the orbital stability of members across the family, thereby enabling the detection of any structural changes, or bifurcations. The figures constructed in this investigation resemble Benest's stability diagrams.[5] However, key differences exist, including: the use of the orbital period as a constant comparable quantity and the application to a wider variety of families. In fact, this investigation examines exclusion plots for the following simply-periodic families at mass ratios in the range, $\mu = [0.1, 0.5]$: Lyapunov orbits about the L_1 collinear equilibrium point; distant retrograde orbits about each primary; distant and low prograde orbits about the larger primary; and retrograde orbits that orbit both primaries. As a comparison to the Sun-planet and planet-moon systems commonly examined in the solar system, as well as binaries with less evenly distributed masses, composite stability representations are extended to include, where applicable, mass ratios in the range $\mu = [1 \times 10^{-6}, 0.1]$.

DYNAMICAL MODEL

To facilitate exploration of the dynamical structure in the vicinity of a binary, the circular restricted three-body problem (CR3BP) is employed. This dynamical model, which serves as a reasonable first approximation to the actual gravitational field, reflects the motion of a massless particle under the influence of the point-mass gravitational attractions of two primaries. By convention, the body of interest, P_3, moves in the vicinity of the larger and smaller primaries, P_1 and P_2, each body P_i possessing a mass m_i. In the CR3BP, a rotating coordinate frame, $\hat{x}\hat{y}\hat{z}$, is introduced and oriented relative to an inertial frame, $\hat{X}\hat{Y}\hat{Z}$. In the frame that rotates with the motion of the two primaries, the location of P_3, measured with respect to the barycenter, is written in terms of the nondimensional coordinates (x, y, z). Length quantities are nondimensionalized such that the distance between P_1 and P_2 is equal to a constant value of one. In addition, time is nondimensionalized such that the mean motion of the primaries is equal to one, while the characteristic mass quantity, m^*, is the sum of the masses of the primaries. The characteristic mass quantity yields nondimensional mass values for P_2 and P_1 equal to μ and $(1-\mu)$, respectively. In the rotating frame, the equations of motion for the spacecraft can be written as:

$$\ddot{x} - 2\dot{y} = \frac{\partial U}{\partial x}, \qquad \ddot{y} + 2\dot{x} = \frac{\partial U}{\partial y}, \qquad \ddot{z} = \frac{\partial U}{\partial z} \tag{1}$$

where the pseudo-potential function, $U = \frac{1}{2}(x^2 + y^2) + \frac{1-\mu}{d} + \frac{\mu}{r}$; then, $d = \sqrt{(x+\mu)^2 + y^2 + z^2}$ and $r = \sqrt{(x-1+\mu)^2 + y^2 + z^2}$. This pseudopotential function can be exploited to develop the energy integral that corresponds to the equations of motion as formulated in the rotating frame. Since the pseudopotential is autonomous, its derivative with respect to time is always equal to zero. A constant energy integral, C, therefore, exists and is equal to:

$$C = x^2 + y^2 + \frac{2(1-\mu)}{r_1} + \frac{2\mu}{r_2} - \dot{x}^2 - \dot{y}^2 - \dot{z}^2 \tag{2}$$

This energy integral is the well-known Jacobi constant in the CR3BP.[6]

In the absence of an analytical solution to the nonlinear differential equations, significant insight into the dynamics in the CR3BP emerges from particular solutions. In this dynamical model, there exist five equilibrium points, labelled L_i, for $i = 1, 2, 3, 4, 5$ and their relative locations are depicted by red diamonds in Figure 1 for a system with a mass ratio of $\mu = 0.3$. Also displayed in this figure are sample zero velocity curves at a Jacobi constant value of 3.885. The gray shaded area represents a forbidden region where a particle would possess an imaginary velocity, while white regions of allowable motion are labelled as displayed in Figure 1. The curve bounding this forbidden region is constructed numerically by the intersection of an infinite set of points that possess a velocity of zero, relative to the rotating frame, with the xy-plane.[4] Within the bounds of these zero-velocity curves, there are infinite possible sets of initial conditions. At various values of the energy constant, four types of steady-state solutions exist: equilibrium points, periodic orbits, quasi-periodic orbits, and chaotic motion.[7] Each of these motions can be examined using concepts developed from dynamical systems theory.[8]

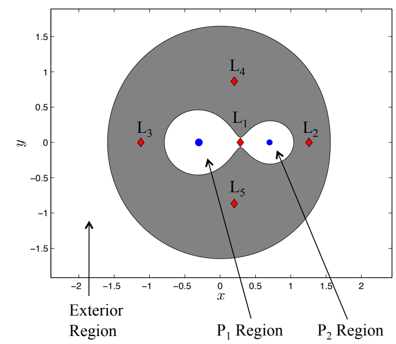

Figure 1: Zero velocity curves in the CR3BP at an energy level C = 3.885 in a system with μ = 0.3.

PERIODIC ORBITS

Of particular interest in this investigation are planar, periodic solutions, which lie within the plane of motion of the two primaries and repeat after a period, T. In fact, the dense set of periodic orbits in the CR3BP, which exist in continuous families, form the underlying structure of the phase space: a stable orbit attracts trajectories in its vicinity, while trajectories near an unstable orbit flow away from the orbit.[12] In the vicinity of stable periodic orbits are quasi-periodic orbits, which trace out the surface of a torus. This boundedness may be approximately retained in a higher-fidelity gravitational environment. Accordingly, the search for stable periodic orbits may be useful in the design of parking orbits for observation of surface activities during a mission to a binary asteroid, for example. Unstable orbits, however, are often utilized as transfer mechanisms between various regions of the phase space. This saddle-like behavior can be exploited during exploratory missions to collect scientific data about both primaries in a binary asteroid system, as well as in modeling the capture or ejection of exoplanets from binary star systems. Thus, identifying periodic orbits and evaluating their stability delivers significant insight into the underlying structures in their vicinity.

Periodic orbits can encircle either one or both primaries in any direction in the rotating frame. For clarity, some definitions are useful. At any instant, a trajectory in the rotating frame with an angular momentum vector with respect to one of the primaries in the $+\hat{z}$ direction is defined as prograde.[4] Correspondingly, a state along a retrograde path possesses an angular momentum vector directed in the $-\hat{z}$ direction. In the rotating frame, a periodic orbit can appear to wind about one of the primaries in an entirely prograde or retrograde direction, or alternate between the two directions as it encircles one or both primaries.

Stability

The stability of a periodic orbit is typically deduced from the monodromy matrix, defined as the state transition matrix (STM) propagated for precisely one period of the orbit.[9] Given a reference planar periodic orbit, the solution that approximates a nearby arc is determined using the linear variational equations of motion. The solution describing the relative neighboring arc is written as $\delta\bar{x}(t) = \mathbf{\Phi}(t, 0)\delta\bar{x}(t_0)$ where $\delta\bar{x}(t_0)$ is the vector variation with respect to the initial state along the orbit and $\mathbf{\Phi}(t, 0)$ is the state transition matrix, essentially a linear mapping from t_0 to a time t.[10] Via Floquet theory, the monodromy matrix of the reference periodic orbit is decomposed into the following form:

$$\mathbf{\Phi}(T, 0) = \mathbf{V}(0)e^{\mathbf{\Omega}T}\mathbf{V}(0)^{-1} \tag{3}$$

where the diagonal elements of $\mathbf{\Omega}$ are the Poincaré exponents, Ω_i, for $i = 1...6$.[10] Since $e^{\mathbf{\Omega}T}$ is a diagonal matrix, $\mathbf{V}(0)$ is a matrix that is formed from the eigenvectors of the monodromy matrix, $\mathbf{\Phi}(T, 0)$, and the

Poincaré exponents are related to its eigenvalues such that $\lambda_i = e^{\Omega_i T}$. The eigenvalues of the monodromy matrix reflect the characteristics of the linear approximation to the dynamics; however, the nontrivial eigenvalues also supply insight into the stability of the original, nonlinear reference solution.

Each planar, periodic orbit, any of which may exist in the full three-dimensional space, possesses a monodromy matrix that can be decomposed into six eigenvalues and their associated eigenvectors.[10] Two of the eigenvalues are equal to unity due to periodicity; the other four nontrivial eigenvalues may be represented in the form $\lambda = a \pm bi$, in terms of two real numbers, a and b. Depending on the value of a and b, three specific types of eigenvalues emerge: real, complex, and imaginary. Regardless of the form of these eigenvalues, however, they appear as reciprocal pairs due to the symplectic properties of the state transition matrix. A stability index is defined as the sum of each pair of reciprocal eigenvalues, equal to $s = \lambda + \frac{1}{\lambda}$.[4] From the Lyapunov definition of stability, a periodic orbit that exhibits stability has a pair of complex or imaginary eigenvalues, $\lambda_1, \lambda_2 = a \pm bi$, and therefore a stability index between $s = -2$ and $s = 2$. A pair of reciprocal eigenvalues, $|\lambda_1| = a > 1$ and $|\lambda_2| = 1/a < 1$, however, correspond to instability.[9] Unstable periodic orbits can, therefore, be identified by at least one stability index with a magnitude greater than two. Since the stability of a planar periodic orbit reflects the behavior of solutions within its vicinity, the parameter s reduces the complexity in visualizing the stability of orbits along a family at various values of the mass ratio.

Bifurcations

In the CR3BP, periodic orbits exist in families that, for a given mass ratio, depend upon the energy constant, C. Varying C, the natural parameter, directly modifies the vector field and, therefore, its infinite set of solutions. A local bifurcation occurs if a change in the energy constant results in a change in the qualitative behavior of trajectories in the vicinity of a periodic orbit. In dynamical systems, a bifurcation may result in a change in the stability of the periodic orbits along a family, the formation of a new family of periodic orbits, or termination of the current family.[11] Since the stability of a periodic orbit reflects the behavior of nearby trajectories, local bifurcations are detected and characterized by monitoring the pairs of nontrivial eigenvalues of the monodromy matrix corresponding to each periodic orbit along a family. Possible bifurcations are detected through changes in the stability of the periodic orbits comprising a family, reflected by the parameter s as it passes through any critical values.

Although many possible bifurcations exist, two types emerge within the dynamical environment that is the focus of this investigation: tangent and period-multiplying bifurcations. A family of periodic orbits undergoes a tangent bifurcation when the qualitative stability characteristics of its orbits change with the energy constant. During this type of local bifurcation, one pair of nontrivial eigenvalues from the monodromy matrix passes through the critical values $\lambda_1 = \lambda_2 = +1$. Simultaneously, the stability index passes through $s = 2$. Depending on the type of tangent bifurcation, the change in stability may be accompanied by the creation of families of similar period or by the intersection with another family of orbits. Across each form of tangent bifurcation, the eigenvalues that reflect the stability of the orbits along a family transition between the unit circle and the real axis. During a period-multiplying bifurcation of multiplicative factor m, a family of period-mq orbits emerges from a family of period-q orbits. Here, q is the integer corresponding to the number of times a periodic orbit encircles a reference location. At the critical value of the natural parameter, the orbit located at the intersection of the two families is equivalently described as a period-mq orbit or a period-q orbit traced out m times. Employing properties of the STM, this bifurcation is detected when the eigenvalues of the period-q orbits along a family pass through the first and $(m-1)$-th complex roots of unity, or, equivalently, when the stability index passes through the critical value, $s = 2\cos\left(\frac{2\pi}{m}\right)$. Since the stability index does not reflect the imaginary components of any complex conjugate eigenvalues, confirmation of a period-multiplying bifurcation requires verification that the eigenvalues do not split off the unit circle after passing through the corresponding roots of unity. Note that the special case of a period-doubling bifurcation occurs when the stability index passes through the critical value of $s = -2$.

Manifolds

Manifold structures departing and approaching unstable periodic orbits can guide the flow in various regions of the phase space, as well as influence the formation and existence of families of periodic orbits. A periodic orbit that is unstable, within or out of the plane, possesses both stable and unstable modes, indicated by the eigenvalues $|\lambda_1| < 1$ and $|\lambda_2| > 1$, respectively. Introducing a small step in the direction of the corresponding eigenvectors at various points along the periodic orbit, the unstable and stable manifold structures are computed by propagating these initial conditions forward or backward in time, respectively.[9] When propagated for a sufficiently long time interval, the resulting manifolds trace out complex paths in the six-dimensional phase space and are usually difficult to visualize over time. Accordingly, manifold structures can generally be adequately represented by their successive intersections with a surface of section, such as the plane $\Sigma : y = 0$ in configuration space. Consider, for example, the manifolds emanating from an unstable L_1 Lyapunov orbit in a system with mass ratio $\mu = 0.26$, as portrayed in Figure 2(a). Stable manifolds, propagated to their first crossing with the $y = 0$ plane, such that $\dot{y} > 0$, are colored blue, while unstable manifolds are colored red, with the primaries indicated by gray diamonds and the L_1 Lyapunov orbit plotted in black. Although the manifolds are only propagated for one return to the surface of section, their representation in configuration space is complex when integrated for a longer time interval. As plotted in Figure 2(b), each manifold crossing of the surface of section defined by $y = 0$ forms a curve in a two-parameter space, such as $(x, \dot{x})$. This reduction in the dimension of the manifolds simplifies visualization of the stable and unstable manifolds associated with the L_1 Lyapunov orbit, and facilitates the examination of the dynamics in the vicinity of the manifolds.

Formation and Existence of Periodic Orbits

Two types of periodic orbit families exist, and are distinguished by their formation process: regular and irregular periodic orbits. As described by Contopoulos, regular orbits are those emerging as a result of bifurcations from a central periodic orbit. Irregular orbits, however, are formed close to the homoclinic tangles corresponding to unstable periodic orbits.[12] Such families are generated at a tangent bifurcation as a pair of stable and unstable periodic orbits. Such knowledge that some families are formed in the complex tangles of periodic orbit manifolds may guide any investigation into the existence of families that do not reduce to a singularity or equilibrium point. Furthermore, this observation suggests that manifolds may also play a key role in governing the evolution of a family.

COMPOSITE STABILITY REPRESENTATION

To visualize the stability of a planar family of periodic orbits across a range of mass ratios, a simple composite representation is constructed using the stability index. At a specified value of the mass ratio, the in-plane and out-of-plane stability indices corresponding to periodic orbits along a family are plotted as a function of a continuously-varying natural parameter. Although it is nonunique, the orbital period serves as an intuitive characteristic quantity. In fact, in the search for exoplanets about binary systems using eclipse-timing or pulse-detection, the period may be the only orbital parameter that can be accurately deduced, to within a multiplicative factor, without significant limiting assumptions. The in-plane and out-of-plane stability indices

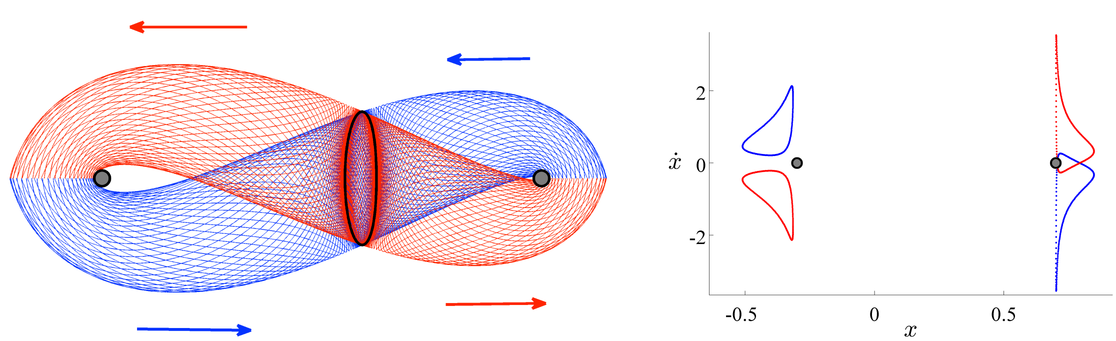

(a) Manifolds in configuration space. (b) Manifold intersections with $y = 0$.

Figure 2: Sample L_1 stable and unstable manifolds.

across a family of orbits at a given mass ratio each form a single curve when plotted against the orbital period. Often, the stability index along these curves exhibits a number of turning points and a large range of values. Simultaneously plotting these complex curves at various values of the mass ratio can hinder any exploration of the stability characteristics along the family. Accordingly, a simplified representation of the stability in a two-parameter space, such as (μ, T), enables clearer visualization, and aids in the examination of the evolution of the family.

The composite stability representation is constructed by simply assessing a qualitative measure of the stability along a family. To demonstrate this process, consider the stability index along the retrograde family of orbits in the exterior region, encircling both primaries, given a mass ratio $\mu = 0.1$. Sample orbits along this family are plotted in Figure 3(a) using three different colors to provide clarity. The direction of motion along these orbits is indicated by an arrow and the primaries are located by gray-filled diamonds. A zoomed-in view of the in-plane stability along this family is displayed on the right in Figure 3(b). As evident from the figure, this family possesses an intricate stability curve. A composite stability representation is then constructed by simply assessing a qualitative measure of the stability along a family. Since the eigenvalues of the monodromy matrix reflect a linear approximation of the dynamics, they can only be used to qualitatively determine the type of stability exhibited by a periodic orbit. In particular, each orbit is classified using the stability index, s: stable, for $s = [-2, 2]$; positive unstable, for $s > 2$; and negative unstable, for $s < -2$. The point representing a single periodic orbit in the two-parameter space, (μ, T), can, therefore, be colored by the type of stability it exhibits. In this investigation, a stable orbit is assigned the color blue, a positive unstable orbit is colored red and negative instability is represented by the color purple. A composite stability representation, for a single value of the mass ratio, appears in Figure 4 to summarize the stability information, with the stable orbits brought to the front of the figure when multiple orbits possess the same period. Through examination of the stability curve, the retrograde exterior family consists of members with each of the three types of stability. Accordingly, at a mass ratio of 0.1, this family will contribute a single line including blue, red and purple points to the composite stability representation, as displayed in Figure 4. Thus, a complex curve encompassing a large range of values of s is reduced to a single line that is overlaid for mass ratios within a specified range, forming a useful composite stability representation. These plots are developed further and examined within the context of two examples.

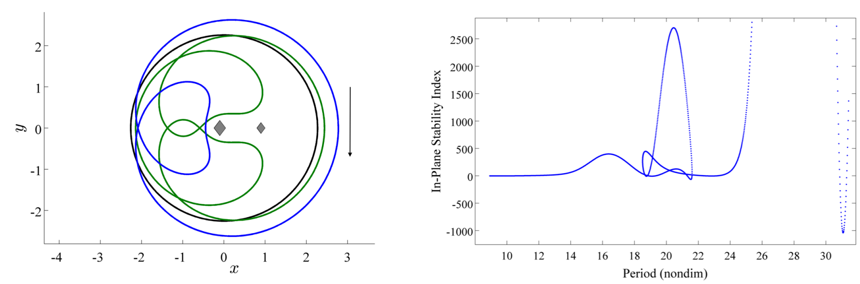

(a) Selected orbits along the retrograde exterior family for a mass ratio of $\mu = 0.10$.

(b) Zoomed-in view of the in-plane stability index along the retrograde exterior family for a mass ratio of $\mu = 0.10$.

Figure 3: Transfer examples.

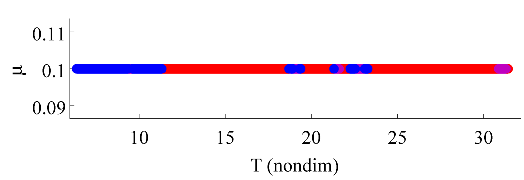

Figure 4: Colored representation of the in-plane stability of the retrograde exterior family at $\mu = 0.10$.

APPLICATIONS OF COMPOSITE STABILITY REPRESENTATIONS

Composite representations of the in-plane and out-of-plane stability indices are employed to examine the evolution with the mass ratio for a variety of simply-periodic families that exist in various regions of the space in the CR3BP. The observations are initially focused on systems with large mass ratios, i.e., within the range $\mu = [0.1, 0.5]$, with additional comparisons made to smaller mass ratios, $\mu = [10^{-6}, 0.1]$, that are indicative of the Sun-planet and planet-moon combinations within the solar system. The composite stability representations for various families are presented within the context of two examples: the search for parking orbits for extended observation of a binary asteroid, and the identification of possible motions of an exoplanet about a binary star system. For the purposes of demonstrating the use of composite stability representations, the focus in both examples is on the search for stable periodic orbits near large mass ratio systems. Since the stability within and out of the plane is decoupled for planar periodic orbits, the two corresponding stability indices are isolated and examined separately. Accordingly, observations on the evolution of the stability of periodic orbits with the mass ratio requires two composite stability representations per family.

Selection of Parking Orbit for Extended Observation of a Binary Asteroid

Recent mission concepts have identified asteroids as a scientifically interesting target for both robotic and manned exploration. Among the large number of asteroids that have been observed, 16% exist in systems consisting of multiple bodies. In fact, many of the binary asteroids that have been discovered possess mass ratios that are much larger than the systems commonly examined within the solar system. In the absence of a close approach to the Earth-Moon system, an accurate determination of the composition and mass distribution of the asteroids in a binary system is often difficult. Accordingly, the mass ratio of a binary asteroid is typically an estimate that may be subject to change as the dynamical and geological environment is better characterized. Prior to sending a spacecraft to the vicinity of a binary asteroid for extended periods of observation and measurement, it may be advantageous to select a type of parking orbit that is stable over a range of mass ratios close to the estimated value. The benefit to preselecting an orbit family that is relatively insensitive in terms of the stability to variations in the mass ratio is that it is simpler to perform smaller adjustments to ensure near-periodicity of a parking orbit in the same family than it is to identify an entirely new type of parking orbit mid-mission. In this example, composite stability representations are employed to identify stable periodic motions near a binary asteroid.

Observation of an Entire Binary Asteroid If both components of a binary asteroid are the subject of observation and measurement, a family of periodic orbits that encircle both primaries in the CR3BP, such as the retrograde orbits that exist in the exterior region, may be examined. This family of orbits is employed to motivate the utility of composite stability representations, and is also used to demonstrate the construction of each plot. The corresponding stability representation for a portion of this family is depicted in Figures 5(a) and 5(b) for the in-plane and out-of-plane stability, respectively. To limit the computational time and effort, only orbits that possess periods below 18 nondimensional time units are sought. Of course, since this is a nonlinear system, the family may possess turning points that introduce stable members with periods less than 18 nondimensional time units. Recall that stable orbits are located within the blue regions of these composite representations, while negative instability is indicated by purple points and positive unstable orbits are located within the red regions. Colored structures, therefore, reflect the stability of periodic orbits along a family, as well as the occurrence of some bifurcations. If the family is closed or reduces to an equilibrium point, for example, these "dynamical barriers" are represented via gray shading, which indicates that the family cannot extend into a particular region of the (μ, T) space. Since the CR3BP is inherently nonlinear, it may not be possible to accurately predict the stability index across any portions of the family that are not computed. Accordingly, any white regions of space, at a given value of μ, indicate that the family is not computed in its entirety. To facilitate comparison of the orbital stability across a large variety of mass ratios, a mixed linear-log scale is employed to represent μ on the vertical axis. Specifically, mass ratios in the range $\mu = [0.1, 0.5]$ are plotted as a linear scale, while mass ratios in the range $\mu = [10^{-6}, 0.1)$ are displayed using a log scale. The boundary between these two scales is indicated by a black dashed line. For comparison, selected systems with a specific mass ratio are also indicated on the plots that represent the three-dimensional stability index, such as in Figure 5(b). In particular, the mass ratio that corresponds to the binary asteroid 809

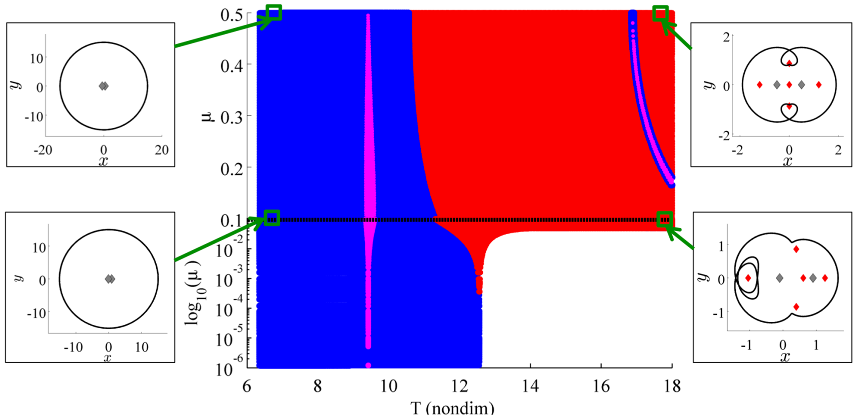

(a) In-plane stability.

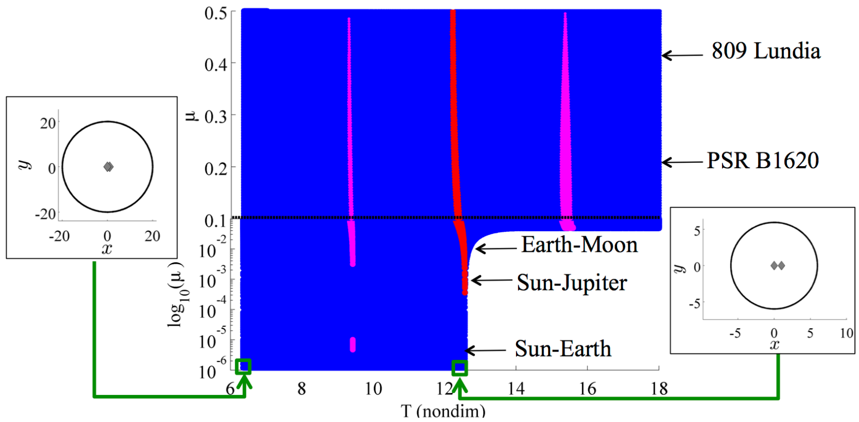

(b) Out-of-plane stability.

Figure 5: Stability representation for the family of retrograde orbits in the exterior region.

Lundia is highlighted on the stability representation. This system, which consists of two V-type asteroids of approximate diameter 6.4 km separated by a distance of 15.8 km, possesses a mass ratio that is approximately equal to 0.41.[13] In addition, the binary star system PSR B1620 is also indicated on the stability representation in Figure 5(b). Consisting of a pulsar and white dwarf separated by a distance of 0.77 AU, this binary system is known to possess a small captured planet. Although the mass ratio of PSR B1620 is not exactly known, it is approximately equal to 0.20.[14] In addition, sample periodic orbits are displayed in the margins at selected mass ratios and periods to reflect the configuration of selected members in physical space.

Using the composite representations presented in Figures 5(a) and 5(b), observations about the stability can be used to assess the sensitivity of the retrograde exterior family of orbits to changes in the mass ratio. First, consider the in-plane stability along this family of orbits. Below periods of approximately 10.5 nondimensional time units, the majority of members of the retrograde exterior family are stable. There does, however, exist a small region of negative instability centered about $T = 9.5$, where the stability curve plunges below $s = -2$, creating two period-doubling bifurcations. Since the blue region to the left of this structure is bound on its other side by a red region, the retrograde exterior family undergoes a variety of planar period-multiplying bifurcations. In addition, as the period of the retrograde exterior family decreases to its limiting value, the stability index approaches a value of $s = +2$. In fact, this family is formed at its minimum period within the homoclinic tangle of the manifolds of the L_2 Lyapunov orbits. At the formation of this family, a branch of stable and unstable orbits is created, as typical in the formation of irregular orbits.[12] Since the

Jacobi constant at the formation of this family is below the value corresponding to L_3, the L_2 manifolds can pass through the L_3 gateway. Accordingly, the homoclinic tangle that forms the retrograde exterior family of orbits may also involve the manifolds of the L_3 Lyapunov orbits. Such a distinction, however, is difficult to visualize at such large energies. Beyond a period of approximately 10.5 time units, the retrograde exterior family is predominantly unstable in the plane of motion of the primaries, for large values of the mass ratio. There is, however, a thin blue and purple structure that indicates the presence of stable members, as the stability curve plunges below $s = -2$. Since this stable region occurs at increasing values of the period as the mass ratio is decreased, this portion of the family is considered sensitive to changes in large values of μ. As the retrograde family of orbits in the exterior region is continued further, turning points occur, which may contribute additional structures to the stability representation in Figure 5(a). For large mass ratios in the range $\mu = [0.1, 0.5]$, Figure 5(b) reflects that members of this family are predominantly stable in a direction that is perpendicular to the plane of motion of the primaries. There are, however, thin structures of negative and positive instability that are embedded within this figure. The presence of these structures, which appear to divide the blue stable regions approximately every 3 time units, indicates that the out-of-plane stability index is oscillatory with respect to the orbital period.

Given the evolution of the retrograde exterior family of orbits over the examined range of mass ratios, as represented by the composite stability representation, the suitability of members of this family for parking orbits during a mission observation phase is assessed. Since small perturbations can influence the motion of a spacecraft both within and out of the plane, both stability indices must be considered simultaneously. Assuming that parking orbits that are stable in the CR3BP are sought, the overlap of blue regions in both Figures 5(a) and 5(b) are identified. Note that the purple regions corresponding to orbits with negative instability for both in-plane and out-of-plane modes occur at similar periods near $T = 9.5$ across the range of mass ratios examined in this investigation. Aside from this small region, orbits in the retrograde exterior family with periods below approximately 10.5 nondimensional time units are, predominantly, stable both within and out of the plane. Such orbits, which exist far from the two primaries, may, therefore, be examined further for extended observation of the two components in a binary asteroid. Recall that one nondimensional length unit is equal to the distance between the two primaries; for 809 Lundia, these retrograde exterior orbits exist over 24 km from the system barycenter. Within the binary environment, orbits that are unstable within the plane of motion of the primaries exist and might be exploited. In fact, previous missions have successfully employed unstable orbits for transfer design. These orbits, located in the red regions of Figure 5(b) at large values of the orbital period, possess stable and unstable manifolds that can potentially facilitate low cost transfers to the P_1 or P_2 regions. Since this unstable region persists over the entire range of large mass ratios, large period retrograde orbits in the exterior region may serve as transfer mechanisms to the interior region for a system with a poorly known mass ratio. Using the composite stability representation presented in this paper, this insight into the stability of a family of orbits can also be obtained rapidly and straightforwardly for multiple candidate binary systems at a variety of inaccurately known mass ratios.

Periodic Orbits Near a Single Component in a Binary Asteroid Retrograde orbits that emanate from the singularity at P_1 also exist and may be useful for further insight into the behavior in the vicinity of one member of a binary pair. This family of orbits, which can grow quite large in size at high orbital periods, exhibits a wide range of values for the in-plane stability index. Composite stability representations for the in-plane and out-of-plane stability indices across this family are plotted in Figure 6. At low periods, these orbits are close to circular with low altitudes, as depicted in the left margins of the stability representations. Note that for the example of the binary asteroid 809 Lundia, its components are separated by a distance of 15.8 km, which represents one nondimensional length unit. Although the small circular orbits plotted on the left of Figure 6(a) may be defined by an altitude lower than the radius of the largest asteroid in 809 Lundia, these orbits may not intersect the surface of a primary body in an alternative system that possesses a similar mass ratio. These smaller orbits are, therefore, retained in the composite stability representation.

As evident by the in-plane stability representation in Figure 6(a), there exists a set of retrograde orbits that are stable at large mass ratios. In fact, the family is formed at the singularity corresponding to the location of P_1, indicating that the stability index approaches the value $s = +2$ as the period decreases. As the period increases, however, the orbits along this family appear more nonlinear in shape, extending further towards P_2

and beyond the locations of the equilateral points L_4 and L_5. At periods close to $T = \pi$, a purple structure corresponding to negative instability appears. The left and right bounds of this purple structure indicate the presence of two planar period-doubling bifurcations at $s = -2$ that exist for mass ratios in the range $\mu = [0.1, 0.5]$. The presence of this purple region at small mass ratios may be related to the appearance of a purple region in the out-of-plane stability representation in Figure 6(b), which occurs at a similar value of the orbital period. The period-doubling bifurcation that occurs in three-dimensional space may influence the flow within the plane, inducing negative instability along the retrograde exterior family at nearby values of the mass ratio. This potential correlation between the two period-doubling bifurcations may cause the stability curve to plunge below the value $s = -2$; such correlation warrants further examination. Increasing the period even further, well beyond the value $T = \pi$, a region of positive instability exists, where the stability index evolves to a value greater than $s = +2$. Within the blue region, a wide variety of period-multiplying bifurcations apparently occur. At these bifurcations, higher-order planar, periodic orbits intersect this family. Such orbits may possess a physical configuration similar to the simply-periodic retrograde orbits about P_1, but with different stability properties that warrant further investigation. Note that at periods larger than $T = 7$ nondimensional time units, the orbits closely approach the smaller primary and are difficult to compute without large computational effort. From the observations using composite stability representations, it is evident that the in-plane stability of the retrograde P_1 family across the range $\mu = [0.1, 0.5]$ is relatively insensitive to changes in the mass ratio. For smaller mass ratios, however, the family becomes predominantly stable within the xy-plane. Over the computed portion of the family, the purple, blue and red structures that exist at larger periods converge as the mass ratio approaches $\mu = 10^{-5}$, which is close to the mass ratio of the Uranus-Titania system. At these smaller mass ratios, the family exhibits more sensitivity in terms of the in-plane stability index than at larger mass ratios.

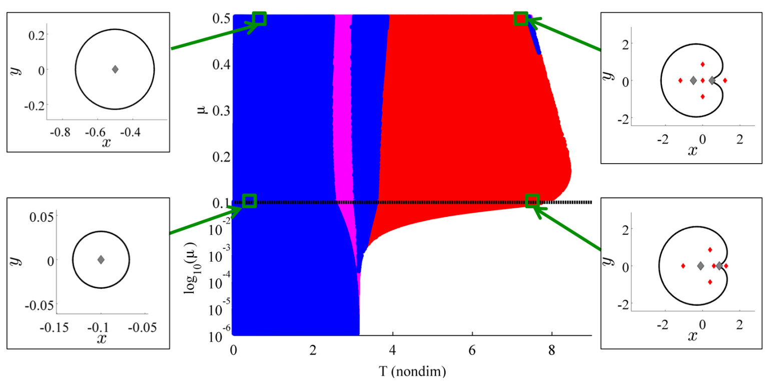

(a) In-plane stability.

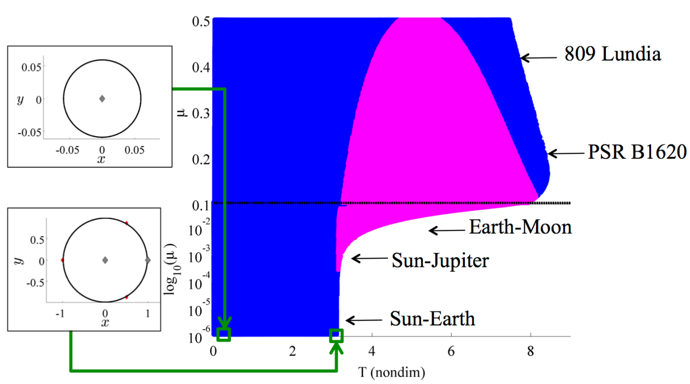

(b) Out-of-plane stability.

Figure 6: Stability representation for retrograde orbits about P_1.

The retrograde family about P_1 exhibits a simple variation in the out-of-plane of stability, as depicted in Figure 6(b). In fact, this figure is predominantly blue with one large purple structure corresponding to negative instability. Accordingly, there are two period-doubling bifurcations that bound this large region and exist for all mass ratios in the range $\mu = [0.1, 0.5]$. The stable region corresponding to smaller periods, therefore, undergoes a wide variety of period-multiplying bifurcations that evolve out of the plane. At smaller mass ratios, below $\mu = 10^{-4}$, which is close to the mass ratio of the Sun-Saturn system, the two period-doubling bifurcations disappear within the range of computable orbits along the family. Thus, for mass ratios smaller than this critical value, the members of this portion of the family appear to be stable. Above this critical value, however, it is evident that, for large periods, the family is quite sensitive to changes in the mass ratio.

Combining the observations from both the in-plane and out-of-plane stability assessments in the retrograde P_1 orbits, portions of this family may be further examined for exploration and scientific observation of a binary asteroid system with an inaccurately known mass ratio. In particular, it is observed that the stable regions of each exclusion plot overlap for periods below approximately 2.5 nondimensional units. Accordingly, orbits with a period below this value exhibit stability in all directions and may be less sensitive to perturbations than larger retrograde orbits. In addition, this region of stability appears to persist across the entire range of mass ratios that appear in Figure 6. For the example of 809 Lundia, where the radius of each body is quite large relative to their separation distance, there are some members of the retrograde family of orbits about P_1 that do not intersect the surface of either primary. At slightly larger orbital periods, just above $T = \pi$ nondimensional time units, there is an additional region of orbits that possesses two stable modes at large values of the mass ratios. However, this region of overlap appears to narrow as the mass ratio is decreased. In any case, the family of retrograde orbits that encircle P_1 are simply represented via composite stability plots, which are used to identify members that are stable both within and out of the plane. Since periodic orbit families vary continuously with both natural parameters - μ and T - the stable retrograde P_1 orbits that possess a given period at nearby values of the mass ratio may appear similar in the phase space.

In the vicinity of the smaller primary, there exist planar orbits that encircle the body in a retrograde direction, commonly denoted the distant retrograde orbits (DROs). At small mass ratios, such as $\mu \approx 0.012$ in the Earth-Moon system, these orbits exhibit in-plane stability across the entire family. Using Figure 7(a) as a reference, it is clear that the stability across the DRO family is more varied for many binary asteroid systems. In particular, for large mass ratios, a purple structure corresponding to negative instability appears near $T = \pi$. This orbital period corresponds to a 2:1 resonance with the period of the primaries. As the value of μ decreases, the two period-doubling bifurcations along the edge of this purple structure occur at larger periods. In addition, the left and right bounds of the purple region merge at a critical value of the mass ratio. This evolution of the period-doubling bifurcations corresponds to the local minimum of the in-plane stability index occurring at less negative values of s, and passing through $s = -2$ at $\mu \approx 0.11$. At this critical mass ratio, the purple structure connects to another structure of negative instability that exists at larger periods, for $\mu > 0.048$. As a reference, this value of μ is larger than the mass ratio corresponding to the Earth-Moon system. Between the two regions of negative instability, the in-plane stability index passes through $s = +2$ twice, creating a large red region of positive instability. As the mass ratio is decreased to a value of $\mu \approx 0.22$, the maximum in the stability index decreases and passes through $s = +2$ as the two tangent bifurcations meet. Below this critical value of the mass ratio, the two tangent bifurcations disappear. Thus, the variation in the in-plane stability index that occurs at large mass ratios is significantly more complex than the stability exhibited by the DROs at the mass ratios for the Sun-planet or planet-moon systems within the solar system.

In contrast to the planar behavior, the out-of-plane stability for orbits in the DRO family is largely homogeneous across all mass ratios. As displayed in Figure 7(b), the out-of-plane stability index predominantly possesses values in the range $s = [-2, +2]$. Noticeably, there is a small region of negative instability at mass ratios close to $\mu = 0.5$, centered at a period of $T \approx 4$. This structure reflects a stability index that plunges below $s = -2$, thereby forming two period-doubling bifurcations. Additionally, a structure corresponding to positive instability appears at small mass ratios below 0.11, for the largest periods along the regions of this family that are computationally reasonable (the maximum period approaches a value close to 2π as $\mu \to 10^{-6}$). This range of μ encompasses the value of μ corresponding to the Earth-Moon system, and many of the Sun-planet combinations in the solar system.

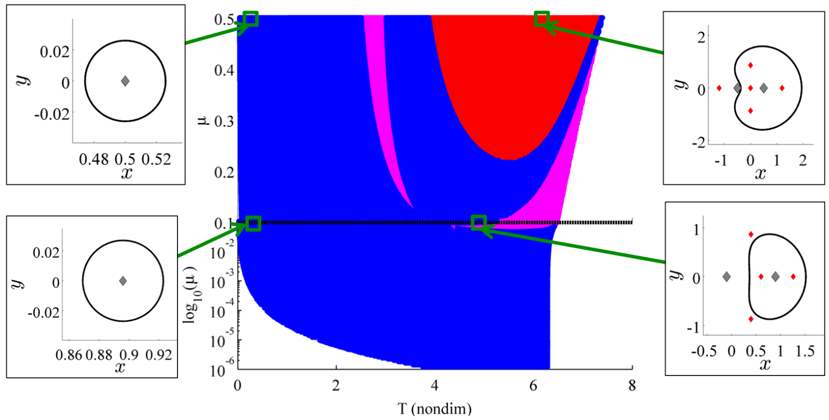

(a) In-plane stability.

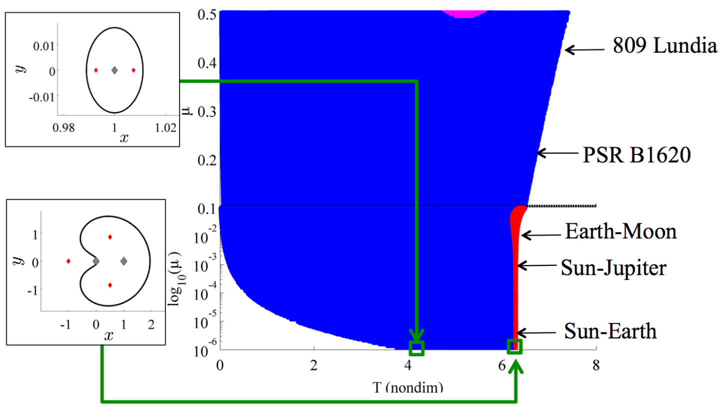

(b) Out-of-plane stability.

Figure 7: Stability representation for retrograde orbits about P_2.

For motion in the vicinity of the smaller primary, the combined stability of the retrograde family of orbits about P_2 is quite useful. Since this orbit family is predominantly stable in the $\hat{z}$ direction, its in-plane stability essentially governs the complete stability of its members. At each value of the mass ratio, large and small, there is a significant range of orbits that are stable in the CR3BP. Depending upon the physical configuration of the components of the desired binary, some of the stable members of this simply-periodic retrograde family of orbits may not intersect or pass too close to the surface of either primary. Such orbits could serve as candidates for further examination in a higher-fidelity gravitational model that also incorporates any eccentricity of the inner binary orbit.

Possible Motions of an Exoplanet About a Binary Star System

In determining potential orbits for an exoplanet within the vicinity of a large mass ratio binary star system, composite stability representations may facilitate the identification of potentially stable periodic motions. Given that it is often difficult to directly observe an exoplanet, the only knowledge of its orbit may be in the form of eclipse timing or variations in the pulses emanating from a pulsar, if present within the binary star system. These observations of the two stars can usually be correlated to an estimate of the orbital period of the exoplanet. Quantification of additional orbital parameters may require the introduction of numerous assumptions based on heuristics. Some orbital quantities may not even be known, such as the inclination of the exoplanet's orbit, which is not resolvable using many of the observation methods commonly employed to detect the possible presence of exoplanets. Since the orbit of an exoplanet may not necessarily trace out a conic, a wide variety of periodic orbits in a three-body gravitational environment may approximately describe its motion. For preliminary identification of potential orbits of an exoplanet for a given value of its period, it is reasonable to assume that if an exoplanet persists along a periodic orbit for an extended period of time, the motion is likely stable. Given this assumption, the search for potential motions of an exoplanet may be guided by the composite stability representations, as demonstrated for simply-periodic prograde motions about the larger primary.

The simply-periodic motion that encircles the larger primary, P_1, includes two families of prograde orbits. These two families, plotted in Figure 8 at a sample mass ratio equal to $\mu = 0.30$, are labelled 'family 1' and 'family 2' in this investigation. The location of the largest primary is marked by a gray filled circle and the direction of motion for both families is indicated by the arrows. Each family evolves with the mass ratio in an intriguing manner that is evident in their composite stability representations and clarified using the stable and unstable manifolds emanating from the L_1 Lyapunov orbits. Assuming the simplified and autonomous dynamical regime described by the CR3BP, composite stability representations are used to identify stable periodic orbits and, subsequently, hypothesize whether such orbits could describe the motion of an exoplanet in the vicinity of a large mass ratio binary star system.

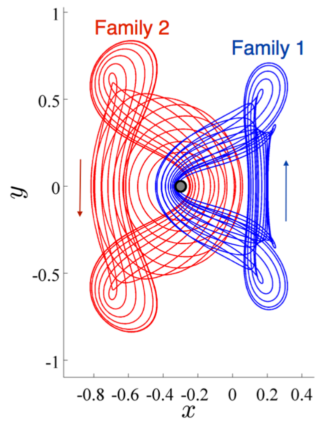

Figure 8: Sample members of prograde orbits in 'family 1' and 'family 2'.

To determine the viability of an exoplanet exhibiting motion corresponding to 'family 1', the evolution of the in-plane stability index over various mass ratios is examined. As evident in the stability representation in Figure 9(a), the family becomes closed (with the upper and lower bounds on the period indicated by the gray shaded regions) and disappears as the mass ratio approaches the value of $\mu \approx 0.26284$. The in-plane stability curves for selected mass ratios close to this critical μ value are plotted as a function of the period in Figure 10, with dotted lines located at $s = +2$ and $s = -2$. In this figure, it is clear that, for each period, two orbits exist in 'family 1'. For a system with a mass ratio of $\mu = 0.27$, stable members of the family exist close to the upper and lower bounds of the period. As the mass ratio is decreased towards the critical value, however, the minimum of the curve rises and passes through $s = -2$. At a nearby value of the mass ratio, the two period-doubling bifurcations at $s = -2$ disappear and result in a stable periodic orbit existing at each value of the period across the family. Thus, small blue structures appear at the bottom of the composite stability representation in Figure 9(a). This family may or may not be closed at all mass ratios; computational difficulties preclude examination of the family as the orbits closely approach P_1 for large mass ratios. Eventually, the two tangent bifurcations at the minimum and maximum period of the family meet, and the family no longer exists. Assuming that the dynamical environment near a binary star system is adequately modeled via the CR3BP, this observation of the disappearance of 'family 1' at the critical μ value suggests that an exoplanet would not exhibit the behavior typical of this family for mass ratios below $\mu = 0.26284$. Since the composite stability representation in Figure 9(a) displays large red regions, this family is predominantly unstable in the plane of motion of the primaries. There is one small blue region corresponding to stable periodic orbits that occur at increasing values of the period as the mass ratio is decreased. In contrast, the composite stability representation in Figure 9(b) reveals that a large portion of the family, with orbital periods above 4.5 nondimensional time units, consists of members that are stable to perturbations that only excite out-of-plane modes. Using the insight gained from the composite stability representation, a small body that is, at some instant, captured in an orbit belonging to 'family 1' is unlikely to persist over long time intervals in the presence of perturbations within the plane of motion of the primaries, or variations in the mass ratio.

The disappearance of 'family 1' at the critical value of the mass ratio, $\mu \approx 0.26284$, is predictable through examination of nearby manifolds. The crossings of the manifolds of the L_1 Lyapunov orbit with the plane

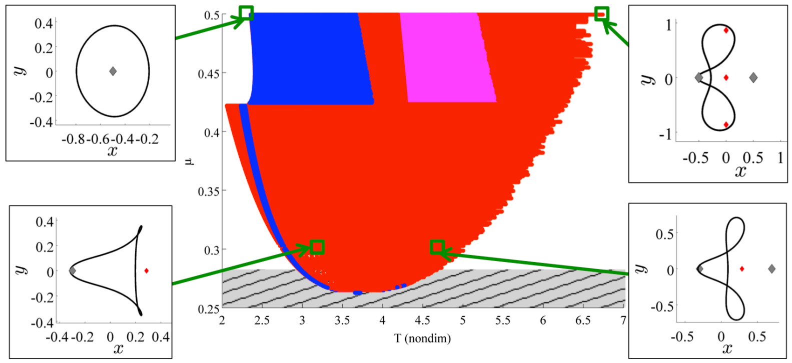

(a) In-plane stability.

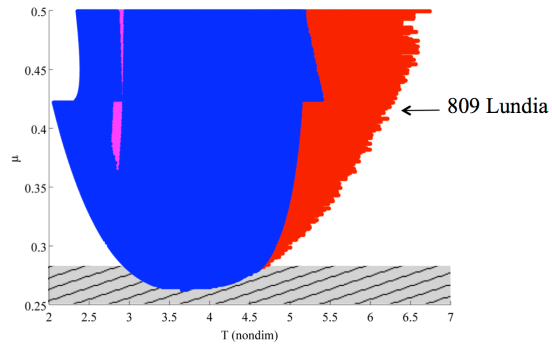

(b) Out-of-plane stability.

Figure 9: Stability representation for 'family 1', comprised of of prograde orbits about P_1.

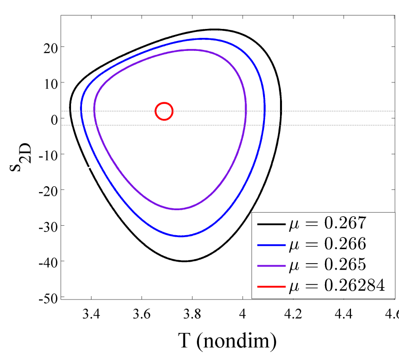

Figure 10: In-plane stability index for 'family 1' at selected values of the mass ratio close to $\mu = 0.26284$.

described by $y = 0$, are plotted in the $(x, \dot{x})$ space in Figures 11(a) and 11(b). These manifolds are computed for a system with mass ratio $\mu = 0.26284$, close to the critical mass ratio, and a Jacobi constant value equal to $C = 3.165$. In Figure 11(a), crossings of the stable manifold with $\dot{y} < 0$ are colored blue, unstable manifold crossings with $\dot{y} < 0$ are colored red, and the black diamond locates P_1. In Figure 11(b), a similar color scheme applies for crossings that posses a positive value of $\dot{y}$. These two zoomed-in views of the manifold crossings appear separately to supply sufficient visual clarity and to separate crossings of the hyperplane in each of the two possible directions. Although the manifold crossings form closed curves, these curves appear to resemble dotted lines of larger spacing with subsequent revolutions of the two primaries. For both of these figures, there are two open circles that are located at similar values of x, with $\dot{x} = 0$, that correspond to the crossings of $y = 0$ for the two periodic orbits in 'family 1' at the specified value of the Jacobi constant. As evident from these two figures, these two periodic orbits are nestled between the stable and unstable manifolds of the L_1 Lyapunov orbits. Accordingly, these manifolds are examined at mass ratios lower than the critical value to explain the disappearance of 'family 1'. Figure 12(a) portrays the stable and unstable manifolds, plotted with the same color scheme as in Figure 11, of an L_1 Lyapunov orbit with Jacobi constant value equal to $C = 3.155$ in a system with mass ratio $\mu = 0.26$. For periodic orbits in 'family 1' to exist at this mass ratio, such an orbit must possess two crossings of the surface of section $y = 0$ with $\dot{x} = 0$ in a similar region along the x-axis. This requirement of two perpendicular crossings corresponds to the symmetry of orbits within this family. It is generally difficult to distinguish the regions which lie within the crossings of a manifold as it encircles the primary. Thus, to search for periodic orbits with such crossings, that also lie close to the manifolds, initial conditions are seeded along the x-axis with $x = [0.15, 0.25]$ and $\dot{x} = 0$. The value of $\dot{y}$ at each point is selected to possess a magnitude that supplies the correct Jacobi constant, and a positive sign to ensure prograde motion about P_1. These initial conditions, plotted as dark gray points in Figure 12(a), are integrated forward in time to their subsequent intersection of the hyperplane $y = 0$. The resulting map crossings, with $\dot{y} < 0$, are also displayed in Figure 12(b) as dark gray points. Note that the curve formed by these crossings does not intersect the hyperplane defined by $\dot{x} = 0$. Accordingly, the manifolds of the L_1 Lyapunov orbit no longer the guide the flow in a manner that allows the symmetric, simply periodic orbits of 'family 1' to exist. Thus, the existence and evolution of this family is governed by the manifolds of the L_1 Lyapunov orbits.

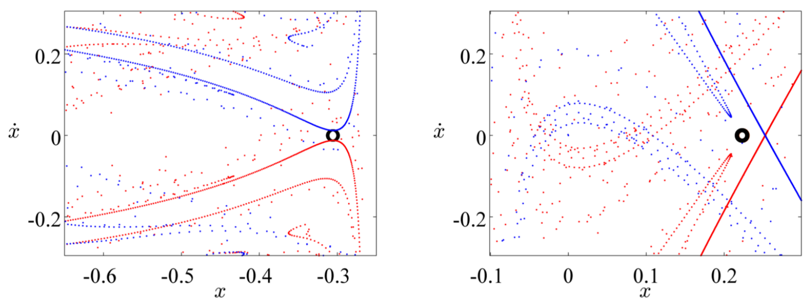

(a) Zoomed-in view of manifold crossings near P_1 with $\dot{y} < 0$.

(b) Zoomed-in view of the manifold crossings near P_1 with $\dot{y} > 0$.

Figure 11: Visualization of flow in the vicinity of the manifolds of the L_1 Lyapunov orbit with $C = 3.165$ in a system with $\mu = 0.26284$ to demonstrate the existence of 'family 1'.

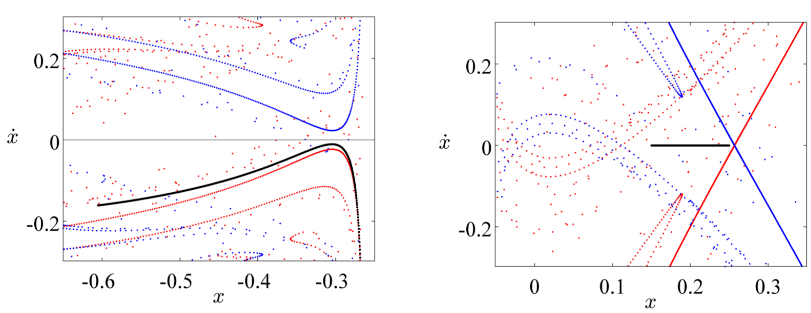

(a) Initial conditions seeded along $y = \dot{x} = 0$, with $\dot{y} < 0$.

(b) First return to $y = 0$, with $\dot{y} > 0$.

Figure 12: Visualization of flow in the vicinity of the manifolds of the L_1 Lyapunov orbit with $C = 3.155$ in a system with $\mu = 0.26$ to demonstrate the disappearance of 'family 1'.

In contrast to the disappearance of 'family 1' at $\mu \approx 0.26284$, 'family 2' continues to exist across the entire range of mass ratios examined within this investigation, and may supply potential orbits to describe the motion of an exoplanet near a binary star system with a mass ratio below this critical μ value. A similar analysis of the manifolds of the L_1 Lyapunov orbits reveals that orbits in 'family 2' are not destroyed at the previously identified critical mass ratio. This observation is straightforwardly visualized using the composite stability representation displayed in Figure 13(a). In particular, this family is predominantly stable within the plane of motion of the primaries with two key purple structures emerging at sufficiently large periods, and meeting at $\mu \approx 0.236$. Recall that these structures represent regions of negative instability and the purple regions in the composite representation are bounded by period-doubling bifurcations. Slightly above the mass ratio $\mu \approx 0.236$, there exists a small oscillation in the in-plane stability index, centered about $s = -2$, that results in three period-doubling bifurcations. As the mass ratio is increased, the oscillation in the stability curve disappears to leave only one period-doubling bifurcation, and only one region of negative instability within the range of computable orbits along the family. The purple structure that exists at smaller periods disappears at $\mu \approx 10^{-3}$, just above the mass ratio of the Sun-Jupiter system. Below this critical value, 'family 2' exhibits stability for both in-plane and out-of-plane behavior. For the out-of-plane stability index, this prograde family of orbits is predominantly stable at large mass ratios. There is, however, one small region of negative instability that occurs just below the resonant period of $T = \pi$, and one small region of positive instability close to $T = 2\pi$. For both stability indices, members of 'family 2' with larger orbital periods display more sensitivity to variations in large values of the mass ratio than the smaller mass ratios

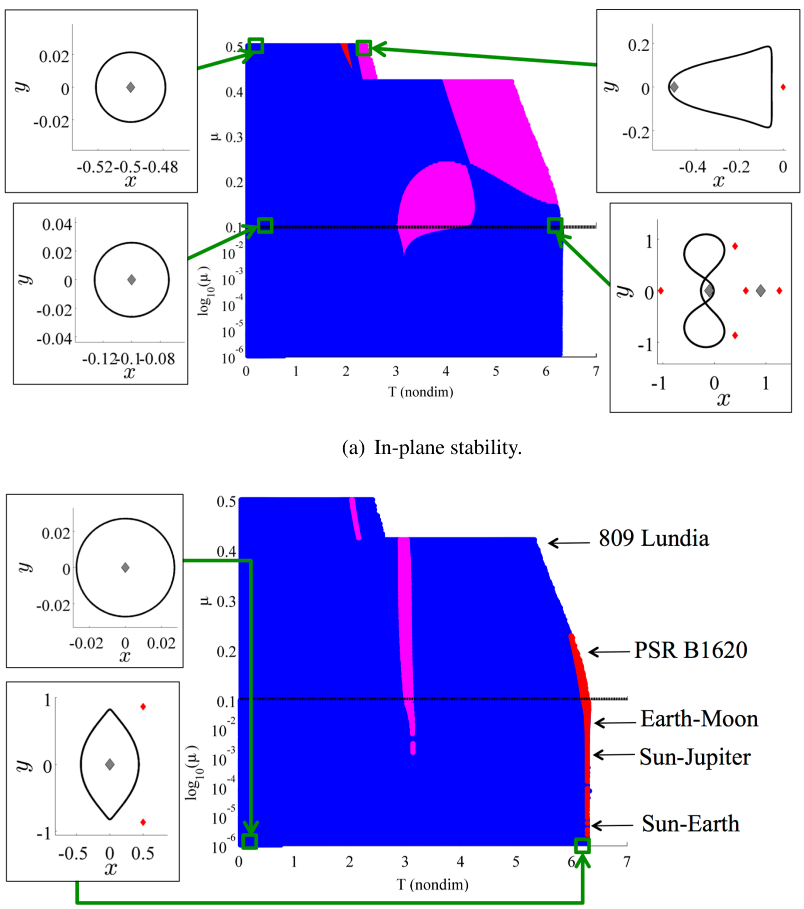

(a) In-plane stability.

(b) Out-of-plane stability.

Figure 13: Stability representation for 'family 2', consisting of prograde orbits about P_1.

corresponding to the Sun-planet combinations within the solar system. At smaller values of the orbital period, however, the composite representation of the orbital stability displays little sensitivity to variations in the mass ratio. In its entirety, the prograde orbits in ‘family 2’, are predominantly stable across the family, both in and out of the plane, and over a range of mass ratios. Since the mass ratio of a binary star system is usually not accurately known, or may change over time due to mass exchange, the composite stability representations reveal that a large portion of this family may supply orbits that could describe the motion of captured small bodies which persist in the vicinity of a binary star system for longer periods of time.

As evident in the composite stability representations, there also exist discontinuities in the stability indices corresponding to ‘family 1’ and ‘family 2’ at a common critical mass ratio. These discontinuities occur at an approximate mass ratio value $\mu = 0.4232$ and, again, appear correlated with the manifolds of the L_1 Lyapunov orbits. First, it is valuable to view the stability curves for ‘family 1’ and ‘family 2’ at mass ratios just above and below the critical value, as plotted in Figure 14. From this figure, it is evident that as the mass ratio passes through the critical value, the two tangent bifurcations at $s = +2$, that occur in each of the two families meet. In fact, in the local neighborhood of the tangent bifurcations in both families, the stability curve appears to resemble a set of ‘asymptotes’ that meet at $s = +2$. For mass ratios below $\mu = 0.4232$, the top two branches of these ‘asymptotes’ are connected to form ‘family 1’, and vice versa for ‘family 2’. As the mass ratio is increased beyond the critical value, ‘family 1’ consists of the two left branches of these ‘asymptotes’, while ‘family 2’ is formed by the righthand ‘asymptote’ branches. This exchange of periodic orbits between ‘family 1’ and ‘family 2’ is reflected by the discontinuities in the in-plane stability index in Figures 9(a) and 13(a). To explain this structural change in the two families, the manifolds of the L_1 Lyapunov orbits are examined at a value of the Jacobi constant equal to $C = 3.61$, which is close to the energy at which the two tangent bifurcations merge. At $\mu = 0.42$, below the critical mass ratio, the stable and unstable manifolds are plotted in blue and red, respectively, in Figure 15(a) for crossings with $\dot{y} < 0$. The crossings of the stable and unstable manifolds with $\dot{y} > 0$ are plotted using the same color scheme in Figure 15(b). In Figure 15(a), purple circles represent the corresponding crossings of three periodic orbits: one that exists in ‘family 2’, and two that exist in ‘family 1’ (one of which possesses a large negative value of s within the plane of motion of the primaries). A set of initial conditions can be seeded along the x-axis of this figure, for the specified value of the Jacobi constant, and propagated forward in time until their next intersection with the $y = 0$ surface of section. The returns to this map are overlaid in gray on Figure 15(b), with intersections of the line $\dot{x} = 0$ indicated by purple circles. Since the resulting curve intersects the x-axis of this figure three times, three symmetric prograde orbits exist at this mass ratio and are nestled between the successive crossings of the manifolds of the L_1 Lyapunov orbit. Using Figure 14 as a reference, it is noted that for a mass ratio above the critical value, e.g., $\mu = 0.43$, only one periodic orbit should exist at $C = 3.61$, with a large negative value of s. This observation reflects the fact that branches of ‘family 1’ and ‘family 2’ have reconnected such that there is a gap between, respectively, the local maximum and local minimum of these two families; this gap appears to be located near $C = 3.61$. A set of initial conditions corresponding to perpendicular crossings of the hyperplane $y = 0$, near the expected locations of the crossings of prograde

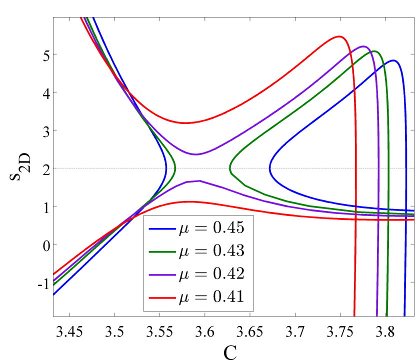

Figure 14: In-plane stability index for ’family 2’ at selected values of the mass ratio close to $\mu = 0.4232$.

periodic orbits, are plotted in Figure 16(a). Upon return to the map, with $\dot{y} > 0$, the resulting crossings form a curve that only intersects the line $\dot{x} = 0$ once. As such, the manifolds of the L_1 Lyapunov orbits no longer guide the flow in their vicinity to produce three symmetric, simply periodic orbits. These dynamics in the vicinity of the manifolds clarify the changes in the structural configuration of both prograde families about P_1 at the observed critical mass ratio. Such exchange of the branches of these prograde families may influence the search for periodic orbits that possess a given orbital period and encircle the larger primary in a binary star system with an inaccurately-known mass ratio near $\mu = 0.4232$.

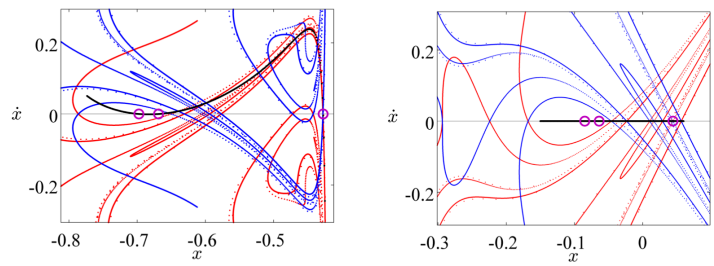

(a) Zoomed-in view of manifold crossings near P_1 with $\dot{y} < 0$.

(b) Zoomed-in view of the manifold crossings near P_1 with $\dot{y} > 0$.

Figure 15: Visualization of flow in the vicinity of the manifolds of the L_1 Lyapunov orbit with $C = 3.61$ in a system with $\mu = 0.42$ to demonstrate the exchange of branches between 'family 1' and 'family 2'.

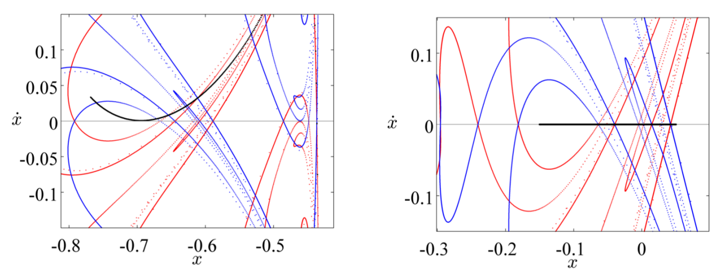

(a) Zoomed-in view of manifold crossings near P_1 with $\dot{y} < 0$.

(b) Zoomed-in view of the manifold crossings near P_1 with $\dot{y} > 0$.

Figure 16: Visualization of flow in the vicinity of the manifolds of the L_1 Lyapunov orbit with $C = 3.61$ in a system with $\mu = 0.43$ to demonstrate the exchange of branches between 'family 1' and 'family 2'.

Another type of periodic motion that could be examined via exclusion plots in the context of binary star systems is the planar family of L_1 Lyapunov orbits. In the Earth-Moon system, these Lyapunov orbits are known to exhibit instability within the plane of motion of the primaries and create three-dimensional orbits, such as the halo and axial families, through bifurcations along the out-of-plane stability index. However, the behavior of the stability indices for large mass ratios appears to exhibit more variability than at the small mass ratios typically examined within the solar system.

The L_1 Lyapunov orbits, which are located between the two primaries, are not solely unstable in the xy-plane for large values of the mass ratio. Using the composite stability representation in Figure 17(a) as a reference, it is evident that for period below 5 nondimensional units, members of the L_1 Lyapunov family possess stabilities with a magnitude greater than two. At larger values of the period, however, the in-plane stability curve plunges into and beyond the range of stability indices $s = [-2, 2]$. Accordingly, a purple region of negative instability appears, and is surrounded by blue regions corresponding to stable orbits. Although computational difficulties prohibit continuation of the entire family, it is likely that unstable orbits also exist at the same periods as the stable orbits. The presence of stable motion near the L_1 gateway may complicate the design of transfers to various regions in the vicinity of a binary with a large mass ratio. Out of the plane of motion of the primaries, however, the stability across the L_1 Lyapunov family is less sensitive to changes in the mass ratio. From Figure 17(b), it is evident that the tangent bifurcations that form the well-known halo and axial families persists for large mass ratios. Additionally, the period doubling bifurcation that occurs at larger values of the orbital period is also present. One notable feature in this composite stability representation is the presence of an additional blue, stable region for mass ratios larger than the value $\mu \approx 0.238$. Above this critical value, the two period-doubling bifurcations approach with increasing values of μ. Combining both the in-plane and out-of-plane stability information for the L_1 Lyapunov family, there are some small regions that indicate the presence of stable orbits. From the computable portions of this family, these regions exist for mass ratios above $\mu = 0.174$ and form small slivers at small periods within the range $T = [5.28, 6.02]$. There is also a small region of total stability corresponding to larger orbital periods. Given that the period corresponding to these small regions evolves with the mass ratio, it is unlikely that an exoplanet could remain in an L_1 Lyapunov orbit for an extended period of time. However, in a binary star system with a poorly known mass ratio, or that is subject to mass exchange, the orbit of an exoplanet may appear temporarily captured in an L_1 Lyapunov orbit, prior to ejection from the system or collision with one of the primaries. Such insight, as gained from the composite stability representations of a variety of families in the CR3BP, may allow for a rapid identification of potential motions of an exoplanet traveling near a low-eccentricity binary star system, thereby guiding more numerically intensive analyses.

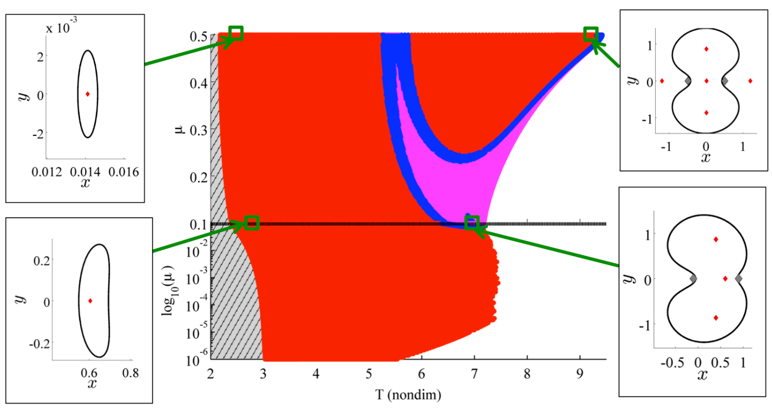

(a) In-plane stability.

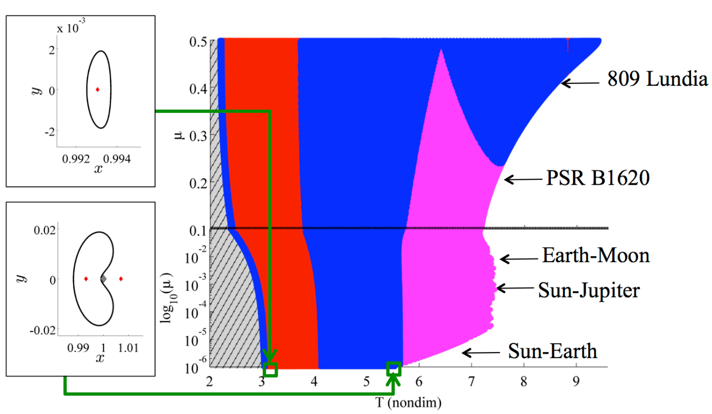

(b) Out-of-plane stability.

Figure 17: Stability representation for L_1 Lyapunov orbits.

CONCLUDING REMARKS

The composite stability representation in this investigation offers a clear and simple method for visualizing the stability of a family of orbits over a range of mass ratios. These figures, which resemble the exclusion plots often employed in physics, allow for the detection of structural changes in a family and an evaluation of the sensitivity of its members to variations in the mass ratio. In particular, such an analysis is completed for the in-plane and out-of-plane stability of a variety of families at large values of the mass ratio, lying in the range $\mu = [0.1, 0.5]$. The results of this analysis are easily comparable to the stability properties of systems with small mass ratios via the composite stability representation. Such observations about the stability of families of periodic orbits may be particularly useful during the design of missions to binary asteroids, or even in the modeling of exoplanet orbits near binary star systems.

ACKNOWLEDGMENT

The authors wish to express their gratitude towards the School of Aeronautics and Astronautics at Purdue University and the Purdue University Lynn Fellowship. In addition, the authors thank AAE Ph.D. student Cody Short for valuable suggestions.

REFERENCES

[1] J.L. Margot, et al. "Binary Asteroids in the Near-Earth Object Population," *Science*, Vol 296 no. 5572, 2002, pp. 1445-1448.

[2] L. Chappaz, K.C. Howell, "Trajectory Exploration Within Binary Systems Comprised of Small Irregular Bodies," *23rd AAS/AIAA Space Flight Mechanics Meetings*, February 2013, Hawaii, AAS 13-414.

[3] E. Fischbach, C.L. Talmadge, *The Search for Non-Newtonian Gravity*, New York: Springer-AIP, 1999.

[4] N. Bosanac, "Exploring the Influence of a Three-Body Interaction Added to the Gravitational Potential Function in the Circular Restricted Three-Body Problem: A Numerical Frequency Analysis", M.S. Thesis, School of Aeronautics and Astronautics, Purdue University, West Lafayette, Indiana, 2012.

[5] D. Benest, "Effects of the Mass Ratio on the Existence of Retrograde Satellites in the Circular Restricted Problem: IV. Three-dimensional Stability of Plane Periodic Orbits," *Astronomy and Astrophysics*, Vol. 54,1977, pp. 563-568.

[6] V. Szebehely, *Theory of Orbits: The Restricted Problem of Three Bodies*. London, UK: Academic Press, 1967.

[7] T.S. Parker, L.O Chua, *Practical Numerical Algorithms for Chaotic Systems*. New York: Springer-Verlag, 1989.

[8] N. Bosanac, K.C. Howell, E. Fischbach, "Exploring the Impact of a Three-Body Interaction Added to the Gravitational Potential Function in the Restricted Three-Body Problem," *23rd AAS/AIAA Space Flight Mechanics Meeting*, February 2013, Hawaii. AAS 13-490.

[9] W. S. Koon, M. W. Lo, J. E. Marsden, S. D. Ross, *Dynamical Systems, the Three Body Problem and Space Mission Design*, 2006.

[10] L. Perko, *Differential Equations and Dynamical Systems*. Third Edition, New York: Springer, 2000.

[11] R. Seydel, *Practical Bifurcation and Stability Analysis: From Equilibrium to Chaos*. New York: Springer-Verlag, 1994.

[12] G. Contopoulos, *Order and Chaos in Dynamical Astronomy*. Germany: Springer-Verlag, 2002.

[13] A. Kryszczynska, F. Colas, P. Descamps, P. Bartczak, M. Polinska, T. Kwiatkowski, J. Lecacheux, R. Hirsch, M. Fagas, K. Kaminski, T. Michalowski, and A. Marciniak, "New binary asteroid 809 Lundia I. Photometry and modelling" *Astronomy and Astrophysics*, Vol. 501, no. 2, 2009, pp. 769-776.

[14] Steinn Sigurdsson, Harvey B. Richer, Brad M. Hansen, Ingrid H. Stairs and Stephen E. Thorsett "A Young White Dwarf Companion to Pulsar B1620-26: Evidence for Early Planet Formation" *Science*, Vol. 301, no. 5630, 2003, pp. 193-196.